The emergence of zonal ocean jets under large-scale stochastic wind forcing

Christopher H. O'Reilly,[1] Arnaud Czaja,[1] and J. H. LaCasce[2]

Received 19 March 2012; revised 9 May 2012; accepted 11 May 2012; published 6 June 2012.

[1] The response of a two-layer quasigeostrophic ocean model to basin scale stochastic wind forcing is investigated. As found in many previous studies, long Rossby waves are excited at the eastern boundary of the square model basin and the waves are baroclinically unstable. A novel aspect we focus on here is that the instability leads to the generation of zonal jets throughout the domain. The jets are actually wave-like in nature, and result directly from the instability. The "jets" appear when averaging the oceanic zonal velocity field over fixed periods of time. The longer the averaging period, the weaker the jets as the latter are in fact time-varying. The jets occur for a wide range of stratification, strength of stochastic forcing and the presence or not of a time mean circulation. The mechanism of jet generation described here thereby provides an explanation for the recent observations of alternating zonal jets in the mid-latitude oceans. **Citation:** O'Reilly, C. H., A. Czaja, and J. H. LaCasce (2012), The emergence of zonal ocean jets under large-scale stochastic wind forcing, *Geophys. Res. Lett.*, *39*, L11606, doi:10.1029/2012GL051684.

1. Introduction

[2] Instantaneous snapshots of the surface flow at mid-latitudes are dominated by mesoscale eddies [e.g., *Chelton et al.*, 2011]. But distinct zonal jets emerge when the flow is averaged over periods up to several years. For example, *Maximenko et al.* [2005, 2008] present evidence of alternating surface-intensified zonal jets in satellite altimetry datasets, with meridional wavelengths of 200–300 km and zonal extents up to an order of magnitude larger.

[3] These observations have rekindled interest in geostrophic turbulence. In the presence of a planetary vorticity gradient, the cascade of energy to larger scales (expected for quasi two-dimensional oceanic flows) is halted in the meridional direction, resulting in zonally elongated eddies [*Rhines*, 1975; *Vallis and Maltrud*, 1993]. The application of this paradigm, or the more recent "PV-staircase" view [*Marcus*, 1993; *Baldwin et al.*, 2007; *Dritschel and McIntyre*, 2008], to oceanic jets is not straightforward though because of the presence of meridional boundaries in ocean basins. In contrast to the situation in zonally periodic domains, the inverse cascade in a bounded basin produces isotropic eddies without zonal jets [*LaCasce*, 2002].

[1]Department of Physics, Imperial College London, London, UK.
[2]Department of Geosciences, University of Oslo, Oslo, Norway.

Corresponding author: C. H. O'Reilly, Department of Physics, Imperial College London, Prince Consort Road, London SW7 2AZ, UK. (christopher.oreilly05@imperial.ac.uk)

[4] In addition to having meridional boundaries, the surface ocean is continually exposed to wind forcing. At mid-latitudes, this comes with the passage of weather systems and with lower frequency shifts in the westerlies, both being essentially stochastic in time beyond timescales of a few weeks. It would seem that such forcing could disturb zonal jets, which are coherent over large distances. But we will show how such forcing can in fact *generate* zonal jet-like structures.

[5] Wind forcing of ocean basins is known to generate long Rossby waves, which emanate from the eastern boundary [e.g., *Gill*, 1982; *Frankignoul et al.*, 1997]. The wave orientation is initially parallel to the boundary, or roughly meridional in many basins. A result is that the waves themselves are baroclinically unstable, because the shear associated with the wave is not zonal [*Rhines*, 1977; *Kim*, 1978; *Jones*, 1979; *Vanneste*, 1995; *LaCasce and Pedlosky*, 2004, hereinafter LP04]. The most unstable wave associated with the instability is nearly zonal due to the planetary vorticity gradient (and thus almost perpendicular to the initial wave). As such, Rossby wave generation can produce features which are very similar to zonal jets.

[6] We test this idea using a two-layer quasi-geostrophic model, forced with a wind pattern mimicking the North Atlantic Oscillation (NAO), the main mode of variability of the jet stream in the North Atlantic [see *Marshall et al.*, 2001]. LP04 identified a parameter, denoted Z, which is the ratio between the time for a Rossby wave (or basin mode) to cross the ocean basin and the e-folding time for unstable growth (which is similar to the *Eady* [1949] time scale). Waves with a small Z are able to cross the basin before succumbing to instability, while those with large Z break up into deformation scale eddies. Here we find, for wind forcing and oceanic stratification typical of the North Atlantic, zonally-elongated baroclinic "tongues" develop on the Rossby waves (large Z limit). These "tongues", when averaged in time, appear as alternating zonal jets, and their presence is robust to changes in basic model parameters and the presence of a time mean circulation.

[7] An alternate explanation for zonal jet formation was proposed recently by *Hristova et al.* [2008] and *Afanasyev et al.* [2011]. In these, an unstable eastern boundary current radiates zonally-elongated disturbances westward. The present mechanism likewise involves baroclinic instability and is thus related.

[8] The note is structured as follows. First, we discuss the setup of the model and the stochastic wind forcing experiments in section 2. Results from the different runs are then presented in section 3 while a discussion of the results follows in section 4.

2. Model

[9] The mechanism described above requires a baroclinic system forced by an imposed wind stress. The simplest such

system is a two-layer quasi-geostrophic basin model. Such a model can capture the instability of baroclinic Rossby waves whilst not overcomplicating the analysis with more detailed stratification. The model is the same as that used by LP04, with Rayleigh dissipation (representing bottom friction) in the lower layer. In addition, we imposed a weaker Rayleigh damping term in the upper layer. The non-dimensional quasi-geostrophic PV equations are

$$\frac{\partial q_1}{\partial t} + J(\psi_1, q_1) + \beta \frac{\partial \psi_1}{\partial x} = W_{Ek} - r_1 \nabla^2 \psi_1, \quad (1)$$

$$\frac{\partial q_2}{\partial t} + J(\psi_2, q_2) + \beta \frac{\partial \psi_2}{\partial x} = -r_2 \nabla^2 \psi_2, \quad (2)$$

where the layer index begins from the surface; ψ_i is the non-dimensional streamfunction; J is the horizontal Jacobian operator; $r_1 = \frac{L}{U}(2800 \text{ days})^{-1}$ and $r_2 = \frac{L}{U}(280 \text{ days})^{-1}$ are the Rayleigh coefficients; W_{Ek} is the surface Ekman pumping due to wind forcing; q_i is the potential vorticity of layer i, defined as:

$$q_i = \nabla^2 \psi_i + h_{3-i} F(\psi_{3-i} - \psi_i), \qquad i = 1, 2, \quad (3)$$

where h_i is the ratio of the layer thickness at rest, H_i, to the total depth ($H_1 = 700$ m, $H_2 = 3300$ m). The non-dimensional parameters β and F are defined, using the reduced gravity g' and the Coriolis parameter $f_0 = 7.3 \times 10^{-5}$ s^{-1}, as

$$F = \frac{f_0^2 L^2}{g' H_1 H_2}(H_1 + H_2) = \frac{L^2}{L_d^2}, \quad (4)$$

$$\beta = \frac{\beta_{dim} L^2}{U}, \quad (5)$$

where the dimensional variables L = 5000 km and U = 0.65 ms^{-1} are the length scale of the basin and characteristic velocity, respectively, L_d = 30 km is the Rossby radius of deformation and $\beta_{dim} = 2.0 \times 10^{-11}$ m^{-1} s^{-1} is the dimensional meridional gradient of the Coriolis parameter.

[10] The form of the Ekman pumping was chosen to represent a simple model of the expansion and contraction of the subtropical and subpolar gyres in the North Atlantic. We model this as a standard double-gyre wind forcing with a single gyre stochastic component to mimic the meridional shifting of the line of zero wind-stress curl associated with the large-scale North Atlantic Oscillation. This is a simplified form of the "Z" shape model used by *Marshall et al.* [2001] to model the effect of the NAO on ocean circulation. The full form of the Ekman pumping is thus:

$$W_{Ek} = W_m \sin\left(\frac{2\pi y}{L_y}\right) + W_s(t) \sin\left(\frac{\pi y}{L_y}\right), \quad (6)$$

where L_y is the meridional scale of the wind forcing, W_m is the (constant) amplitude of the mean double-gyre Ekman pumping and W_s is the stochastic amplitude of the superimposed single-gyre pattern.

[11] The stochastic time series, W_s, is taken from a first order Markov process with zero mean. We used the NCEP/NCAR reanalysis [*Kalnay et al.*, 1996] daily surface wind stress dataset over the North Atlantic to calculate a time series for the large-scale Ekman transport between 27.5°N and 52.5°N over 30 years. The annual cycle was removed to give a time series of the basin-scale Ekman transport anomaly associated with the NAO. The resulting time series was then scaled to have a variance ($\sigma_{ref} = 6.4 \times 10^{-7}$ ms^{-1}) matching that taken from the same dataset, whilst the mean wind amplitude, $W_m = 1.6 \times 10^{-6}$ ms^{-1}, was taken to be equal to a maximum mean Ekman pumping of 50 m yr^{-1} [*Levitus*, 1982].

[12] A prominent feature in turbulent QG basin simulations on the β-plane is the spin-up of inertial recirculation ("Fofonoff") gyres in the north and south of the basin [e.g., *Bretherton and Haidvogel*, 1976; *Salmon et al.*, 1976; *Griffa and Salmon*, 1989; *Wang and Vallis*, 1994; *Özgökmen and Chassignet*, 1998; *Dukowicz and Greatbatch*, 1999; *LaCasce*, 2002]. Such gyres occur even when there is stochastic forcing with zero time mean. Physically, the gyres are the result of the systematic erosion of the background PV gradient by eddies. Likewise, we obtained significant Fofonoff gyres in the simulations with the stochastic forcing. The gyres grew to fill nearly the entire basin. To stem this growth then, we imposed thin dissipative sponge layers in the north and south of the basin. The sponge layers relax the potential vorticity, through an additional $-\gamma q_i$ term on the right hand side of (1) and (2), towards the local planetary vorticity. The timescale of the damping parameter γ was set to 60 days. As the wind forcing was applied away from the sponge layers (L_{sp} = 250 km) in the simulations, this effectively shortened the meridional length (L_y = 4500 km) of the basin.

[13] One may question the extent to which the sponge layers affect the interior dynamics. However, we found that sponge layers were not necessary when the forcing also has a mean component (because the Fofonoff gyres were much weaker). So those simulations were made without sponge layers. Comparing the results suggests the impact on the interior was relatively slight.

[14] The bottom friction parameter was chosen to be $(280 \text{ days})^{-1}$ for all simulations, following other QG simulations of mid-ocean eddies [e.g., *Arbic and Flierl*, 2004]. We tested the sensitivity of the results presented below, to a range of values between $(5400 \text{ days})^{-1}$ and $(60 \text{ days})^{-1}$ and also without bottom friction. The behaviour was insensitive to the exact value used in the stochastic forcing simulations.

[15] All simulations were integrated for 150 years, starting with a resting ocean, and results were taken after the model had equilibrated after a spin-up time of 35 years. We consider first the case with only stochastic wind forcing. Then we examine the case with both mean and stochastic wind components applied.

3. Results

3.1. Stochastic-Only Forcing

[16] After the initial application of the stochastic forcing to the basin, baroclinic and barotropic Rossby waves are seen emanating from the eastern boundary. The barotropic Rossby waves transit the basin in a few days, but the baroclinic Rossby waves have a transit time of about 8 years in the model. As a result, the baroclinic Rossby waves dominate the response of the basin on timescales of months and greater. After 2–3 baroclinic Rossby transit times resonant basin modes, similar to those described by *LaCasce* [2000]

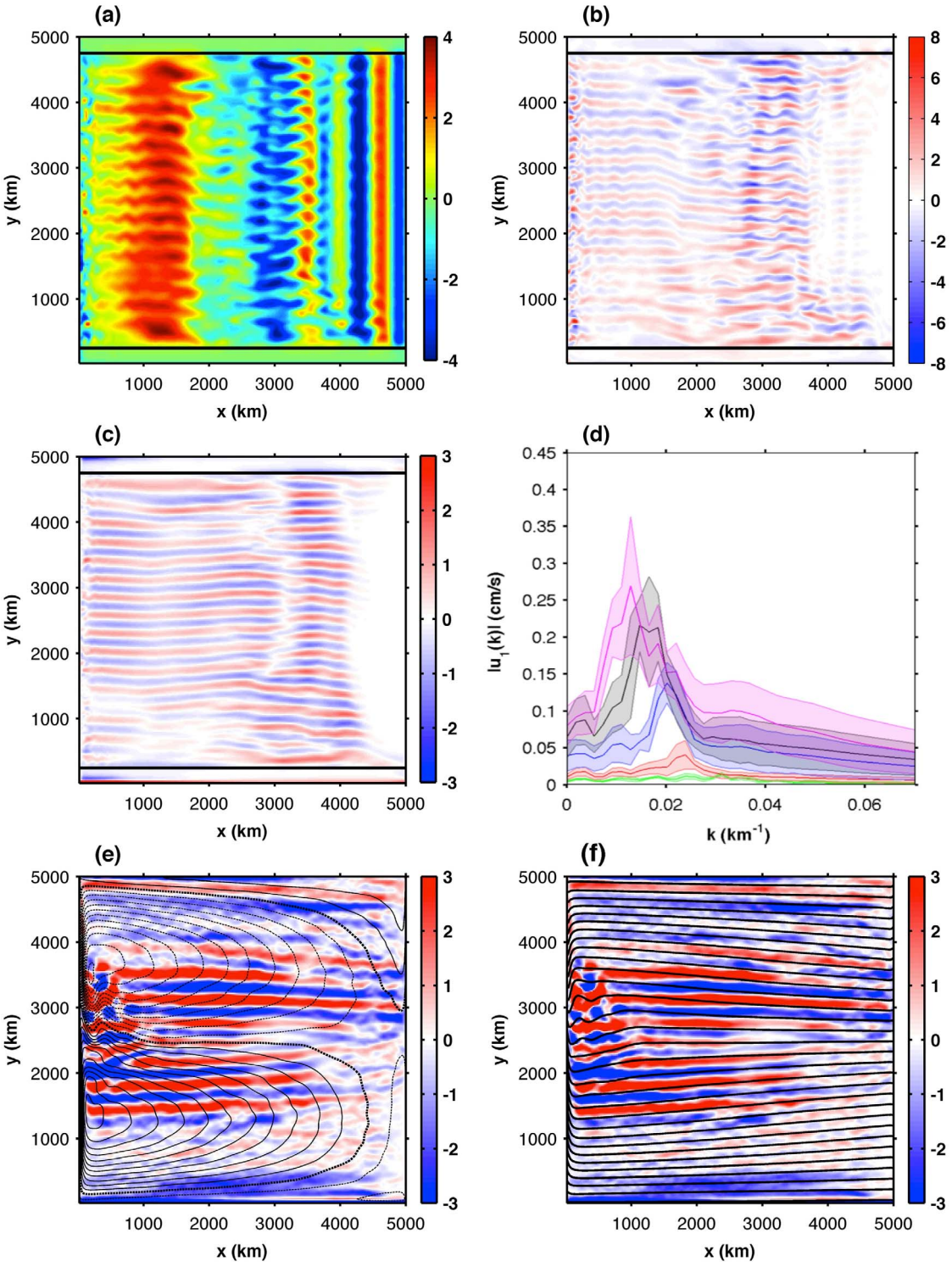

Figure 1. (a) Snapshot of the non-dimensional baroclinic streamfunction in the reference stochastic forcing experiment. Maps of the upper-layer zonal velocity anomaly, u_1' (cm/s), in the stochastic forcing simulation for (b) snapshot and (c) 200-week average. The bold black lines mark the edge of the sponge layers. (d) Wavenumber spectra of the 200-week mean upper-layer velocity anomaly in the stochastic forcing simulations using $\sigma_{W_s} = \sigma_{ref}$ (blue), $\sigma_{W_s} = 0.2\sigma_{ref}$ (green), $\sigma_{W_s} = 0.4\sigma_{ref}$ (red), $\sigma_{W_s} = 2.5\sigma_{ref}$ (black) and $\sigma_{W_s} = 5\sigma_{ref}$ (magenta). The shaded area shows the standard deviation of the independent spectra used to produce each mean spectrum. Maps of the upper-layer zonal velocity anomaly, u_1' (cm/s), in the stochastic forcing simulation for 200-week average with (e) the mean upper-layer streamfunction and (f) mean lower layer PV contours. $\overline{\psi_1}$ is plotted with a contour interval of 5×10^4 m^{2}s^{-1} and the dashed and solid contours denote negative and positive values respectively.

and *Cessi and Primeau* [2001], emerge as the dominant baroclinic waves. These have wavelengths that fit into the basin an integer number of times (i.e., $\lambda = L_x/n$).

[17] Previously, the focus of baroclinic Rossby wave instability studies was the spin-down problem [e.g., *Rhines*, 1977; LP04]. But we also observe wave instability, despite the presence of surface forcing. The instability can be thought of as a triad interaction, between the original baroclinic wave, a second baroclinic wave and a barotropic wave [*Jones*, 1979; *Vanneste*, 1995; LP04]; The latter waves grow at the expense of the potential energy of the primary wave. The barotropic wave in particular has a small zonal wavenumber—it is a wave, but it has a large zonal extent. In the model fields, one observes long zonal "tongues" of energy.

[18] The latter are shown in Figure 1a, a snapshot of the baroclinic streamfunction in the stochastic forcing simulation. The zonal tongues extend from the crest to the trough of the basic (meridionally-orientated) Rossby waves, which remain distinct. Note that the primary waves maintain their North-South alignment because the deformation radius doesn't vary with latitude (although it is possible to allow for this effect in primitive equation models [e.g., *Isachsen et al.*, 2007]. The whole system, including the large-scale meridional wave and the zonal tongues, transit the basin together, until they reach the western boundary. This is what one would expect for a triad of mutually-interacting waves. As the primary wave progresses westward, the zonal perturbations intensify, eventually becoming strong enough to distort the baroclinic field.

[19] This distortion is seen clearly at the surface. In the two-layer model the upper-layer streamfunction represents the surface motion and is related to the barotropic and baroclinic modes by

$$\psi_1 = \psi_{bt} + h_2\psi_{bc}, \tag{7}$$

where ψ_{bt} and ψ_{bc} are, respectively, the barotropic and baroclinic streamfunctions. In particular, the zonal jets emerge when averaging the surface streamfunction, as the primary wave has shorter time scales. Figures 1b and 1c show zonal velocity maps from a snapshot and a 200-week average respectively. The emergence of alternating zonal velocity jets in the 200-week maps is striking.

[20] The jets in Figure 1 have a dominant meridional scale and one expects that this is set by the most unstable meridional wavenumber of the wave instability. For a free Rossby wave in an infinite domain (from LP04), this scale is proportional to the deformation radius. Figure 1d shows the meridional wavenumber spectra of the 200-week average of zonal surface velocity, averaged over 10 independent periods, for five different levels of forcing (prescribed as the standard deviation of $W_s(t)$). The blue line in Figure 1d is the mean zonal surface velocity spectrum of the reference run shown in Figures 1a–1c. The peak of the spectrum was used to determine the dominant meridional scale of the jets. We repeated the simulation with a range of deformation radii (L_d = 20–100 km) and found the dominant wavelength of the emerging jets to scale fairly uniformly with L_d (not shown).

[21] The finite amplitude zonal perturbations have a significant baroclinic component, due most likely to the bottom friction which preferentially damps the deep flow. As such, the zonal jets themselves could be baroclinically unstable. In the two-layer model there is a critical velocity shear for zonal flows below which instability cannot grow [*Phillips*, 1954]. The shear of the jets is consistently close to this threshold. As such, if there is unstable growth on the jets, it is unlikely to occur to a significant degree while the waves cross the basin. But if the jets had stronger shear, we would expect to observe more unstable growth and more turbulent behaviour. To test this hypothesis we repeated the same stochastic experiment but with the standard deviation of $W_s(t)$ 2.5 times larger and 5 times larger than the reference simulation.

[22] The meridional wavenumber spectra for the increased forcing simulations are plotted in Figure 1d; these were calculated in the same way as the spectrum of the reference simulation. The peak velocities increase with the forcing amplitude, as one would expect since the velocity shear of the Rossby waves increases. The spectral peak also shifts to smaller wavenumbers, indicating an increase in the dominant meridional scale of the upper-layer zonal velocity.

[23] LP04 found that increasing the amplitude of the primary wave (their parameter, Z) has a negligible effect on the most unstable wavenumber. However it does increase the unstable growth rate, and also increases the amount of available potential energy in the primary wave field. In their numerical simulations, LP04 found that with large Z waves, an inverse energy cascade followed the instability. This in turn produced larger eddies. The shift toward smaller wavenumbers seen in Figure 1d reflects a similar effect.

[24] Interestingly, an inverse cascade should favor the barotropic mode, but we find that a significant amount of kinetic energy remains in the baroclinic mode, even in the 200-week averages. One explanation is that having a thinner upper layer hinders the transfer of energy to the barotropic mode [*Fu and Flierl*, 1980; *Smith and Vallis*, 2002; *Scott and Arbic*, 2007]. Bottom friction however has a similar effect [e.g., *LaCasce and Brink*, 2000], and this could also be the cause. In any case, the present experiments suggest that the forcing amplitude affects the scale of the jets, albeit weakly, increasing it beyond the deformation radius predicted by linear theory.

[25] But there is a limit. Increasing the amplitude to 20 times the reference value results in no discernible jets. In this case the resulting eddy field is largely barotropic *and* isotropic. This is the limit considered by *LaCasce* [2002] and seen also by LP04.

[26] For completeness, the simulation was performed with smaller values of the forcing and as before their meridional wavenumber spectra are plotted in Figure 1d. The baroclinic Rossby waves generated by the weaker stochastic forcing have weaker shear and the initial unstable growth is slower. This is clear from the very small peak in the $\sigma = 0.4\sigma_{W_s}$ simulation and the lack of an obvious peak in the $\sigma = 0.2\sigma_{W_s}$ spectrum, where there is no significant instability growth on the Rossby waves in the basin transit time.

3.2. Mean and Stochastic Forcing

[27] Now we examine the response with a mean double gyre wind forcing applied in addition to the NAO-type stochastic wind forcing–see equation (6). Figure 1e is a plot of the surface zonal velocity anomaly (defined as the departure from the 115 year mean field), averaged over 200-weeks.

The mean wind generates the familiar double gyre circulation, but the alternating zonal jets are again clearly visible, extending across the gyres (note that unlike in the purely stochastic wind forcing experiments (Figures 1a–1d), time averaging really is needed for the jets to emerge in presence of a mean circulation as the development of the instability is masked by the gyre-scale flow and barotropic waves). The jets are most prominent in regions where the mean flow is eastward shown (Figure 1e), or opposite to the direction of Rossby wave propagation (indeed barotropic velocities and long Rossby wave phase speed are comparable for the control parameter values). An eastward barotropic flow slows the baroclinic wave transit across the basin, allowing more time for the instability to develop. Where the mean flow is westward (in the north and south of the basin), the Rossby wave speeds are augmented and the instability has less time to act.

[28] Interestingly, the meridional scale of the jets increases westwards, where the flow, near the separated boundary currents, is more turbulent. The amplitude of the jets also increases in this region, suggestive of an inverse cascade of energy.

[29] Another aspect, in contrast to the previous case, is that the jets appear to tilt in the interior. This effect stems from the distortion of the PV contours by the mean flow. Figure 1f shows the zonal velocity anomaly averaged over 200-weeks plotted against contours of the mean lower-layer PV, $\overline{q_2}$, given by

$$\overline{q_2} = \beta y + h_1 F \overline{\psi_{bc}}. \tag{8}$$

The mean flow distorts the contours of $\overline{q_2}$ from βy (latitude lines), tilting them in the direction of the mean flow. The lower-layer of the model is unforced, so time-averaged fluid motion in the lower layer is constrained by the $\overline{q_2}$ contours. This is not the case in the upper layer, where the wind forcing permits motion across the $\overline{q_1}$ contours. The emerging jets in Figure 1f seem to follow the $\overline{q_2}$ contours in the interior. They deviate somewhat, approaching the western boundary where the flow is more turbulent and the variability of $q_2(t)$ is larger.

4. Summary and Discussion

[30] Our QG simulation of basin-scale stochastic forcing with zero time mean, a simple model of the NAO, produces zonal jet structures similar to those recently found in observations. In these simulations, the wind forcing excites baroclinic Rossby waves emanating from the eastern boundary. As these propagate westward they become unstable, producing a secondary wave with long zonal extent. If one averages the surface fields in time, the latter appear as distinct, alternating jets. In most cases, the meridional scale of the jets is set by the most unstable meridional wavelength of the instability, which scales with the deformation radius. However with stronger forcing, the unstable growth rate is larger and the resultant eddy field is more energetic. This can lead to an inverse energy cascade, increasing the dominant length scales.

[31] The alternating zonal jets are also found when a mean component of the winds is added to the stochastic forcing. The former generates a double gyre system with their associated western boundary currents. The mean gyres affect the jet formation by altering the propagation speed of the primary baroclinic waves. Where the mean flow is eastward, the waves are slowed, allowing more time for the instability to grow. The gyres also modify the orientation of the jets, by deforming the PV contours in the lower layer. The jets are then approximately aligned with those contours. A similar tilting was observed by *Maximenko et al.* [2008].

[32] An important distinction exists between the jet-like features observed in our basin simulations and the β-plane jets found in a periodic domain [*Rhines*, 1975; *Vallis and Maltrud*, 1993]. The latter span the domain zonally, like the rings of Jupiter. The "jets" seen here are in fact *waves*, with long zonal scales. Averaging the fields in time blurs the zonal dependence, giving them the appearance of jets. But averaging them over progressively longer times weakens their signature. With infinite averaging times, the features necessarily disappear. As a result, a finite averaging period is key to the meridional arrangement of zonal instability "tongues" giving rise to alternating bands of zonal velocity.

[33] We note that the mechanism described here is likely to have a strong dependence on latitude. The parameter Z, the ratio of the transit time of the baroclinic Rossby wave to the Eady growth time, varies inversely with the third power of the deformation radius, with larger values to the north (LP04). At low latitudes Z is small and the Rossby waves can transit the basin before succumbing to instability while at high latitudes, where Z is large, the response is more turbulent [*Isachsen et al.*, 2007]. So the present mechanism is most likely relevant at mid-latitudes.

[34] Thus, Rossby wave instability is a possible explanation for quasi-zonal jets in the ocean. As noted though, an unstable eastern boundary current can produce similar features [*Hristova et al.*, 2008; *Afanasyev et al.*, 2011]. Such currents are precluded in our idealized model set-up. It is likely that both mechanisms are at play in the ocean, with the present one producing jets in the interior and the boundary currents producing them in the eastern part of the domain.

[35] **Acknowledgments.** Christopher H. O'Reilly was funded by a Natural Environment Research Council bursary. We thank Peter Rhines and Mike Spall for constructive reviews of the first draft.

[36] The Editor thanks two anonymous reviewers for assisting in the evaluation of this paper.

References

Afanasyev, Y., S. O'Leary, P. Rhines, and E. Lindahl (2011), On the origin of jets in the ocean, *Geophys. Astrophys. Fluid Dyn.*, *106*(2), 113–137.

Arbic, B., and G. Flierl (2004), Baroclinically unstable geostrophic turbulence in the limits of strong and weak bottom ekman friction: Application to midocean eddies, *J. Phys. Oceanogr.*, *34*(10), 2257–2273.

Baldwin, M., P. Rhines, H. Huang, and M. McIntyre (2007), The jet-stream conundrum, *Science*, *315*(5811), 467–468.

Bretherton, F., and D. Haidvogel (1976), Two-dimensional turbulence above topography, *J. Fluid Mech.*, *78*, 129–154.

Cessi, P., and F. Primeau (2001), Dissipative selection of low-frequency modes in a reduced-gravity basin, *J. Phys. Oceanogr.*, *31*(1), 127–137.

Chelton, D., M. Schlax, and R. Samelson (2011), Global observations of nonlinear mesoscale eddies, *Prog. Oceanogr.*, *91*, 167–216.

Dritschel, D., and M. McIntyre (2008), Multiple jets as PV staircases: The Phillips effect and the resilience of eddy-transport barriers, *J. Atmos. Sci.*, *65*(3), 855–874.

Dukowicz, J., and R. Greatbatch (1999), Evolution of mean-flow Fofonoff gyres in barotropic quasigeostrophic turbulence, *J. Phys. Oceanogr.*, *29*(8), 1832–1852.

Eady, E. (1949), Long waves and cyclone waves, *Tellus*, *1*(3), 33–52.

Frankignoul, C., P. Müller, and E. Zorita (1997), A simple model of the decadal response of the ocean to stochastic wind forcing, *J. Phys. Oceanogr.*, *27*, 1533–1546.

Fu, L., and G. Flierl (1980), Nonlinear energy and enstrophy transfers in a realistically stratified ocean, *Dyn. Atmos. Oceans*, *4*(4), 219–246.
Gill, A. (1982), *Atmosphere-Ocean Dynamics*, *Int. Geophys. Ser.*, vol. 30, Academic, New York.
Griffa, A., and R. Salmon (1989), Wind-driven ocean circulation and equilibrium statistical mechanics, *J. Mar. Res.*, *47*(3), 457–492.
Hristova, H., J. Pedlosky, and M. Spall (2008), Radiating instability of a meridional boundary current, *J. Phys. Oceanogr.*, *38*(10), 2294–2307.
Isachsen, P., J. LaCasce, and J. Pedlosky (2007), Rossby wave instability and apparent phase speeds in large ocean basins, *J. Phys. Oceanogr.*, *37*(5), 1177–1191.
Jones, S. (1979), Rossby wave interactions and instabilities in a rotating, two-layer fluid on a beta-plane, *Geophys. Astrophys. Fluid Dyn.*, *12*(1), 1–33.
Kalnay, E., et al. (1996), The NCEP/NCAR 40-year reanalysis project, *Bull. Am. Meteorol. Soc.*, *77*(3), 437–471.
Kim, K. (1978), Instability of baroclinic rossby waves; energetics in a two-layer ocean, *Deep Sea Res.*, *25*(9), 795–814.
Lacasce, J. (2000), Baroclinic rossby waves in a square basin, *J. Phys. Oceanogr.*, *30*, 3161–3178.
LaCasce, J. (2002), On turbulence and normal modes in a basin, *J. Mar. Res.*, *60*(3), 431–460.
LaCasce, J., and K. Brink (2000), Geostrophic turbulence over a slope, *J. Phys. Oceanogr.*, *30*(6), 1305–1324.
LaCasce, J., and J. Pedlosky (2004), The instability of Rossby basin modes and the oceanic eddy field, *J. Phys. Oceanogr.*, *34*, 2027–2041.
Levitus, S. (1982), *Climatological Atlas of the World Ocean*, *NOAA Prof. Pap.*, *13*, 173 pp.
Marcus, P. (1993), Jupiter's great red spot and other vortices, *Annu. Rev. Astron. Astrophys.*, *31*, 523–573.
Marshall, J., H. Johnson, and J. Goodman (2001), A study of the interaction of the North Atlantic Oscillation with ocean circulation, *J. Clim.*, *14*, 1399–1421.
Maximenko, N. A., B. Bang, and H. Sasaki (2005), Observational evidence of alternating zonal jets in the world ocean, *Geophys. Res. Lett.*, *32*, L12607, doi:10.1029/2005GL022728.
Maximenko, N. A., O. V. Melnichenko, P. P. Niiler, and H. Sasaki (2008), Stationary mesoscale jet-like features in the ocean, *Geophys. Res. Lett.*, *35*, L08603, doi:10.1029/2008GL033267.
Özgökmen, T., and E. Chassignet (1998), Emergence of inertial gyres in a two-layer quasigeostrophic ocean model, *J. Phys. Oceanogr.*, *28*(3), 461–484.
Phillips, N. (1954), Energy transformations and meridional circulations associated with simple baroclinic waves in a two-level, quasi-geostrophic model, *Tellus*, *6*(3), 273–286.
Rhines, P. (1975), Waves and turbulence on a beta-plane, *J. Fluid Mech.*, *69*(3), 417–443.
Rhines, P. (1977), The dynamics of unsteady currents, in *The Sea*, vol. 6, *Marine Modeling*, edited by E. D. Goldberg et al., pp. 189–318, John Wiley, New York.
Salmon, R., G. Holloway, and M. Hendershott (1976), The equilibrium statistical mechanics of simple quasi-geostrophic models, *J. Fluid Mech.*, *75*(4), 691–703.
Scott, R., and B. Arbic (2007), Spectral energy fluxes in geostrophic turbulence: Implications for ocean energetics, *J. Phys. Oceanogr.*, *37*(3), 673–688.
Smith, K., and G. Vallis (2002), The scales and equilibration of midocean eddies: Forced-dissipative flow, *J. Phys. Oceanogr.*, *32*(6), 1699–1720.
Vallis, G., and M. Maltrud (1993), Generation of mean flows and jets on a beta plane and over topography, *J. Phys. Oceanogr.*, *23*, 1346–1346.
Vanneste, J. (1995), Explosive resonant interaction of baroclinic Rossby waves and stability of multilayer quasi-geostrophic flow, *J. Fluid Mech.*, *291*, 83–108.
Wang, J., and G. Vallis (1994), Emergence of Fofonoff states in inviscid and viscous ocean circulation models, *J. Mar. Res.*, *52*(1), 83–127.